RESEARCH ARTICLE
Cytoskeleton, September 2010 67:599–607 (doi: 10.1002/cm.20470)


# Tropomyosin Is a Tetramer Under Physiological Salt Conditions

Ingrid Lassing,[1]* Louise Hillberg,[2] Anna-Stina Höglund,[1] Roger Karlsson,[1] Clarence Schutt,[3] and Uno Lindberg[2]

[1]*Department of Cell Biology, The Wenner-Gren Institute, Stockholm University, Stockholm, Sweden*
[2]*Department of Microbiology, Tumour Biology and Cell Biology, Karolinska Institute, Stockholm, Sweden*
[3]*Department of Chemistry, Princeton University, Princeton, New Jersey*

Received 25 January 2010; Revised 2 June 2010; Accepted 6 July 2010
Monitoring Editor: Bruce Goode

**Tropomyosin (TM) is a coiled-coil dimer of α-helical peptides, which self associates in a head- to-tail fashion along actin polymers, conferring stability to the microfilaments and serving a regulatory function in acto-myosin driven force generation. While the major amount of TM is associated with filaments also in non-muscle cells, it was recently reported that there are isoform-specific pools of TM multimers (not associated with F-actin), which appear to be utilized during actin polymerization and reformed during depolymerization. To determine the size of these multimers, skeletal muscle TM was studied under different salt conditions using gel-filtration and sucrose gradient sedimentation, and compared with purified non-muscle TM 1 and 5, as well as with TM present in non-muscle cell extracts and skeletal muscle TM added to such extracts. Under physiological salt conditions TM appears as a single homogenous peak with the Stokes radius 8.2 nm and the molecular weight (mw) 130,000. The corresponding values for TM 5 are 7.7 nm and 104,000, respectively. This equals four peptides, implying that native TM is a tetramer in physiological salt. It is therefore concluded that the TM multimers are tetramers.** © 2010 Wiley-Liss, Inc.

**Key Words:** tropomyosin assembly, ionic strength dependence, microfilament organization, actin polymerization, cell motility

## Introduction

Activation of the force-generating actin microfilament system is a key event in cell migration of non-muscle cells. The complex molecular mechanism which directs external signals into control of the formation of membrane lamella and microspikes [Chinkers et al., 1979; Mellstroom et al., 1983], and eventually leads to translocation of whole cells has been subject of extensive research during a long period of time. The first step in this process; the polymerization of actin at the fast growing (+)-ends of filaments, juxtaposed to the plasma membrane [Wang, 1985; Lai et al., 2008], occurs in immediate conjunction with stimulation of cells through membrane bound receptors, acting via the phosphatidyl-inositol (PtdIns)-cycle and small GTPases [(Lassing and Lindberg, 1988; Brachmann et al., 2005; Hall, 2005)]. During the last decade several complex molecular machineries involved in filament formation have been disclosed [Goley and Welch, 2006; Renault et al., 2008], the most well characterized of which are the members of the WASP/Wave, formin and Ena/Vasp families of proteins [Goley and Welch, 2006; Takenawa and Suetsugu, 2007; Le Clainche and Carlier, 2008]. The involvement of redox processes in the control of the microfilament system has also been recognized [Sundaresan et al., 1995; Fratelli et al., 2002; Dalle-Donne et al., 2003; Moldovan et al., 2006; Chiarugi and Fiaschi, 2007; Lassing et al., 2007]. The controlled accessibility of filament (+)-ends for incorporation of actin monomers derived from the profilin:actin (P:A) complex, is a key event for polymerization to occur and involves capping protein [Mejillano et al., 2004] and the gelsolin family of proteins [Silacci et al., 2004]. Members of the formin family of proteins act as processive polymerases incorporating actin from P:A whilst remaining bound at the (+)-end of the filaments [Carlier and Pantaloni, 2007; Renault et al., 2008]. Recently, the function of tropomyosin (TM), in the regulation of the actin filament (+)-end has received increased attention [Hillberg et al., 2006; Wawro et al., 2007; Grenklo et al., 2008; Bach et al., 2009; Skau et al., 2009].

Classically, TM participates in the calcium control of acto-myosin force generation in the muscle, yet it is an abundant multi-isoform protein in non-muscle cells, see [Gunning et al., 2005, 2008]. The isoforms are classified into two groups based on their polypeptide length; the low molecular weight (LMW; 247 amino acid residues and mw 28,000), and the high molecular weight (HMW; 284 residues and 32,000) isoforms. The polypeptides fold into elongated

*Address correspondence to: Ingrid Lassing, Department of Cell Biology, The Wenner-Gren Institute, Stockholm University, SE-106 91 Stockholm, Sweden. E-mail: ingrid.lassing@wgi.su.se
Published online 23 July 2010 in Wiley Online Library (wileyonlinelibrary.com).

α-helical structures and these assemble in-register into asymmetrical coiled-coil dimers, commonly of homo-dimer type in non-muscle cells [Gimona et al., 1995]. The dimers bind along the helical grooves of the actin filament in a head-to-tail fashion, conferring stability to the actin filaments against severing activities by cofilin and gelsolin [Ishikawa et al., 1989; Nyakern-Meazza et al., 2002; Ono and Ono, 2002]. Tropomyosin dissociates gelsolin:actin complexes in vitro, leading to filament formation [Ishikawa et al., 1989; Nyakern-Meazza et al., 2002]. Recent evidence implicate a close relationship between TM and activation of formin-dependent elongation at the (+)-end of actin filaments [Evangelista et al., 2002; Wawro et al., 2007; Skau et al., 2009]. The isoform composition of TM in combination with the isoform variation of actin, which in non-muscle cells is present in β- and α-isoforms, can confer functional specializations of the microfilament system [Creed et al., 2008].

It was recently shown that while the major fraction of TM is connected with the insoluble actin cytomatrix, about 10% of the TM appears in soluble, isoform-specific structures present in protruding lamellipodia of spreading cells, where short TM isoforms were most prevalent in the regions closest to the plasma membrane [Hillberg et al., 2006]. Analysis of cell extracts showed that these structures appears as actin-free multimers of TM [Grenklo et al., 2008]. Stimulation of cells with serum causes a rapid actin polymerization accompanied by a decrease of TM1 and TM4 multimers, respectively, which is followed by a pronounced increase in non-polymerized actin as well as the TM multimers. Hence, it was suggested that the multimers serve as assembly intermediates, used in the formation of lamellipodia [Grenklo et al., 2008; Lindberg et al., 2008].

It was demonstrated already in 1948, by Bailey that at low salt concentration TM can form polymers in the absence of actin filaments, and that these polymers are easily disassembled to dimers upon the addition of salt [Bailey, 1948]. The presence of TM multimers in cell extracts, appearing as actin-free distinct peaks, obtained by size chromatography, indicates alternate organisation forms of TM [Grenklo et al., 2008]. This raises a question about the molecular weight of the TM multimers, and the necessity to establish their homogeneity and composition under physiological salt conditions, and therefore prompted the present determination of the molecular weight of TM multimers under physiological salt conditions. The result implies that native TM consists of two dimers, i.e. is a tetramer in vivo.

## Materials and Methods

### Chemicals and Antibodies

Mouse monoclonal antibody TM 311 recognizing TM 1, 2, 3 and 6 was from Sigma-Aldrich, and rabbit polyclonal antibodies to TM 4 (cat no. AB5449) also recognizing TM1 was from Millipore. Pan-reactive mouse anti-actin (clone 4) LMAB-C4 was from Seven Hills. Horseradish-peroxidase (HRP)-conjugated anti-mouse and anti-rabbit IgG, and protein standards for gel filtration were from GE Healthcare. Protein standard Dual Color (#161-0374) for SDS-PAGE was from BioRad. All chemicals were of analytical grade and, unless otherwise stated, purchased from Sigma-Aldrich.

### Protein Purification

Rabbit skeletal muscle TM was purified as described [Smillie, 1982] and stored at −20°C. To avoid oxidation 20 mM dithiotreitiol (DTT) was added upon thawing. The purity of the protein was analysed by SDS-PAGE (12.5%) according to [Laemmli, 1970] and stained with Coomassie brilliant blue. High molecular weight aggregates of TM were removed by sequential ammonium sulphate (AS) precipitation. Pellets containing pure TM were dissolved in 2 mM Tris-HCl pH 8.0 with 50 mM DTT and dialysed in 10 mM $KPO_4$ pH 7.4, 1 mM DTT with either 20 mM KCl, or 150 mM KCl. Vectors containing HA–tagged rat non-muscle TM cDNA were kindly provided by Dr. M Gimona [Gimona et al., 1995]. *E. coli* expressed non-muscle TM-1 and TM-5 was prepared as previously described [Hillberg et al., 2006].

### Cell Culture and Preparation of Cytosolic Extracts

Rat mammary tumour (MTLn3) cells (generously provided by Dr. J. Condeelis) were cultured and extracted as described in [Grenklo et al., 2008] with 1% Triton X-100 in 100 mM NaF, 50 mM KCl, 2 mM $MgCl_2$, 1 mM EGTA, 10 mM $KPO_4$, pH 7.5, 0.5 M sucrose, supplemented with PMSF and water-soluble proteases, to avoid the partial depolymerization of actin often seen with other buffers [Blikstad and Carlsson, 1982].

### Determination of Molecular Weight

The mw of elongated molecules can be determined by combining their Stokes radius ($R_s$) and sedimentation coefficient (S) [Siegel and Monty, 1966]. Gel filtration chromatography was performed using a Superose 6 column [Grenklo et al., 2008]. Sample volume was 0.1 ml unless otherwise indicated, flow rate was 0.4 ml/min and fraction volume was 0.4 ml. The column ($V_0$ = 7.8 ml and $V_t$ = 23.5 ml) was calibrated using globular protein standards, with known $R_s$. Sedimentation coefficients for TM were determined using sucrose density gradient centrifugation [Martin and Ames, 1961]. Briefly samples (0.41 ml) were loaded on 10 ml of a 5–20% (w/v) sucrose gradient (made in buffers as indicated) and with a 0.4 ml cushion of 50% sucrose at the bottom of each gradient. Catalase (S = 11.4) was added as an internal standard and ultracentrifugation L-60 Beckman using a swing-out rotor (SW41) was performed at 25,000 rpm for 25 h at 20°C. Approx. 35 fractions were collected and the catalase position was determined according to [Martin and Ames, 1961]. Tropomyosin positions were assessed by SDS-PAGE and Western blot analysis, S was determined using $S_x = 11.4x(V_t-V_x)/(V_t-V_{cat})$, and the molecular weight was calculated ($M_x = 4205xR_sS_x$), where *x* refers to the specific

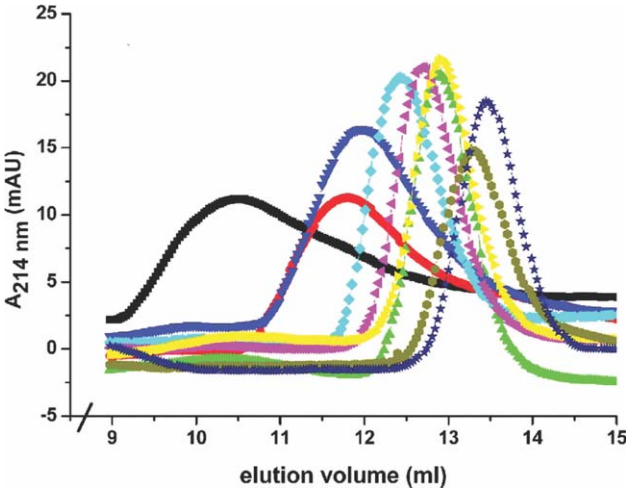


**Fig. 1. Effect of ionic strength on the chromatographic behaviour of skeletal muscle TM.** Samples of skTM in 10 mM $KPO_4$ pH 7.4, 20 mM KCl and 1 mM DTT, were incubated on ice for 2 h at different ionic strengths ($I$ = 0.03–3.0 M) and then chromatographed on Superose 6 (sample volume = 100 µl). Running buffers: 5 mM $KPO_4$ pH 7.4, and 1 mM DTT (I 0.03 M, black curve); 10 mM $KPO_4$ pH 7.4, 1 mM DTT (I 0.06 M, red); 10 mM $KPO_4$ pH 7.4, 10 mM KCl, 1 mM DTT (I 0.07 M, blue); 10 mM $KPO_4$ pH 7.4, 40 mM KCl, 1 mM DTT (I 0.1 M, light blue); 10 mM $KPO_4$ pH 7.4, 80 mM KCl, 1 mM DTT (I 0.14 M, magenta); 10 mM $KPO_4$ pH 7.4, 150 mM KCl and 1 mM DTT (I 0.21 M, green); 10 mM $KPO_4$ pH 7.4, 150 mM KCl, 5 mM $MgCl_2$ and 1 mM DTT (I 0.22 M, yellow); 10 mM $KPO_4$ pH 7.4, 2 M KCl and 1 mM DTT (I 2.06 M, olive) and 0.5 M $KPO_4$ pH 7.4, and 1 mM DTT (I 3.0 M, dark blue).

protein (TM isoform) under study and cat to catalase [Siegel and Monty, 1966].

### SDS-PAGE and Western Blot Analysis

Samples were prepared and analysed as described in [Grenklo et al., 2008] except that 3% bovine serum albumin (BSA) in TBST (100 mM Tris-HCl, pH 8.0, 150 mM NaCl and 0.25% Tween 20) was used for blocking and dilution of antibodies.

## Results

To determine the size of the TM multimers, we used rabbit skeletal muscle TM and compared the results obtained with non-muscle TM isoforms. First, the homogeneity of TM was studied at different ionic strengths and $R_s$ was determined at the corresponding conditions. Aliquots of TM were incubated in phosphate buffer supplemented with increasing concentration of KCl, and subsequently chromatographed on Superose 6 (Fig. 1). The elution profiles showed clear ionic strength dependence; at the lowest ionic strength (5 mM phosphate buffer) a broad peak with a trailing shoulder suggested extensive heterogeneity of TM-assemblies. With increasing ionic strength the elution profile gradually became more Gaussian, indicating increasing homogeneity of the TM complexes formed. The positions of the peaks were gradually shifted towards lower $R_s$, with increasing ionic strength (Table I). At physiological salt concentration (Fig. 1, green curve) the peak appeared at the position corresponding to $R_s$ 8.2 nm, and the bandwidth was as narrow as for thyroglobulin, implying that the molecular organization of TM was homogenous under these conditions, in contrast to the heterogeneous appearances at the lower ionic strengths. As the ionic strength was increased further, the peaks again became broader and shifted towards lower $R_s$, (Fig. 1 and Table I). Including 5 mM $Mg^{2+}$ in the physiological buffer had no effect on the elution profile (Fig. 1, yellow and green curves).

To further study the tendency of TM to organize into different assemblies under different ionic conditions, the homogeneity and $R_s$ were then determined for samples of the protein at a higher concentration (peak fraction $A_{214}$ = 600 compared to 22) and under three different buffer conditions, (Figs. 2A–2C). This confirmed the previous result of a homogenous protein organization with $R_s$ 8.2 nm at physiological conditions, as well as the presence of different assembly forms at low and high salt.

Next, the sedimentation coefficient for TM assemblies obtained at physiological ionic strength was determined in order to calculate the molecular weight. Two samples of TM from the peak fraction after chromatography at physiological salt were prepared (Fig. 2A); one was left untreated, while the other was incubated with formaldehyde prior to centrifugation to avoid possible disintegration of TM organisation during subsequent sedimentation through the 5–20% sucrose gradient in 10 mM $KPO_4$ pH 7.4, 150 mM KCl. As shown in (Figs. 3A and 3B), sedimentation profiles of fixed and unfixed TM were nearly superimposed indicating a stable organisation of TM at physiological ionic conditions. In both cases TM appeared exclusively in a few fractions only (Fig. 3A). Of these the position of the meniscus [Siegel and

**Table I. Stoke's Radius ($R_s$) of Skeletal Muscle Tropomyosin at Different Ionic Strengths (I)**

| Buffer | I (M) | $R_s$ (nm) |
|---|---|---|
| 5 mM $KPO_4$ pH 7.4 | 0.03 | n.d. |
| 10 mM $KPO_4$ pH 7.4 | 0.06 | 9.2 |
| 10 mM $KPO_4$ pH 7.4, 10 mM KCl | 0.07 | 9.2 |
| 10 mM $KPO_4$ pH 7.4, 40 mM KCl | 0.10 | 8.7 |
| 10 mM $KPO_4$ pH 7.4, 80 mM KCl | 0.14 | 8.4 |
| 10 mM $KPO_4$ pH 7.4, 150 mM KCl | 0.21 | 8.2 |
| 10 mM $KPO_4$ pH 7.4, 150 mM KCl, 5 mM $MgCl_2$ | 0.225 | 8.2 |
| 10 mM $KPO_4$ pH 7.4, 2 M KCl | 2.06 | 7.6 |
| 0.5 M $KPO_4$ pH 7.4 | 3.0 | 7.5 |

All buffers were supplemented with 1 mM DTT.

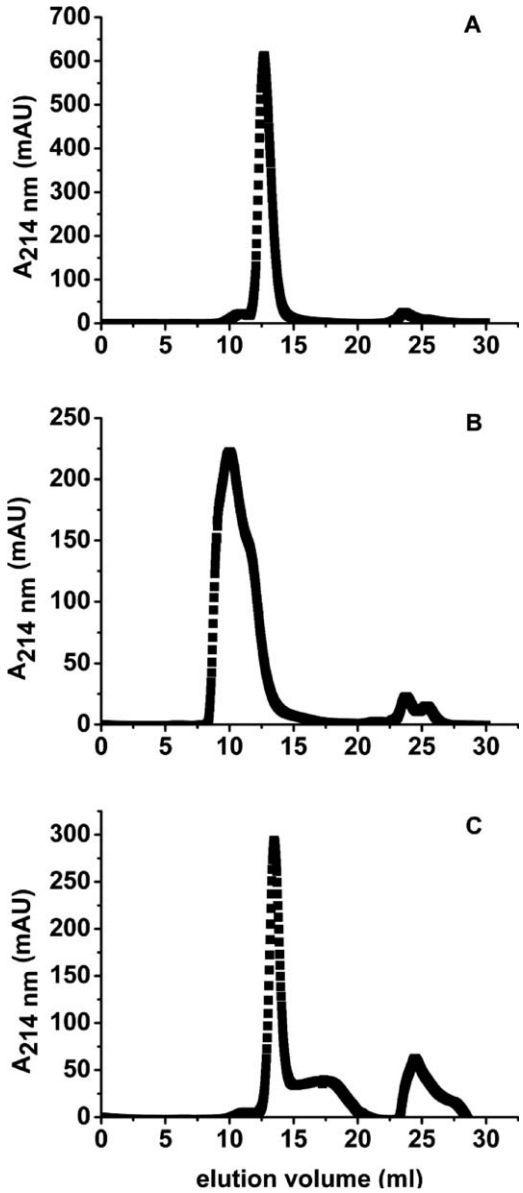


**Fig. 2. Homogeneity of skTM under physiological (A), low (B) and high (C) salt conditions.** skTM from a concentrated stock was subjected to gel filtration on Superose 6 in 10 mM $KPO_4$ pH 7.4, 150 mM KCl and 1 mM DTT (A); in 10 mM $KPO_4$ pH 7.4, 1 mM DTT ( B); and in 0.5 M $KPO_4$ pH 7.4, 1 mM DTT (C), see legend to Figure 1 for experimental details.

Monty, 1966], results in the sedimentation coefficient 3.8, and combined with the corresponding $R_s$ (8.2 nm; Table I) a molecular weight of 130,000 was calculated (see Methods) for both the unfixed and fixed protein. This value corresponds to four TM chains, (32,000) and it is thus concluded that the native TM molecule is a tetramer under physiological salt conditions. This was further corroborated by SDS-PAGE analysis of the fixed and unfixed material from the two sedimentations, where fixed TM appeared at a position close to 120,000, and the unfixed protein migrated to the monomer position (Fig. 3D). Notably by increasing the sample boiling time, the intensity of the band at 120,000 decreased and a band at the monomer position appeared instead, reflecting four TM molecules in the upper band, which dissociate due to the fact that formaldehyde fixation is not stable under conditions used for preparation of samples for SDS-PAGE. Also the fractions corresponding to the lowest S-value (2.5) contained tetramers as judged from the SDS-PAGE (Figs. 3A and 3D).

The salt dependent variations in $R_s$ of TM (Fig. 1 and Table I) implied that there were differences in the organisation of TM, either in the number of assembled TM molecules or in the assembly mode (i.e staggered, end to end, or bundled). To determine the molecular weight of the TM assemblies obtained at a low (I = 0.06 M, 10 mM $KPO_4$) and high (I = 3.0 M, 0.5 M $KPO_4$) ionic strength sucrose gradient sedimentations were performed under these conditions. At the low ionic strength $R_s$ was 9.2 nm, and the major amount of TM appeared at a position corresponding to an S-value of 4.2 (Fig. 3C, and Table II), resulting in the mw of 160,000. This result is in accordance with the previous molecular weight determination using light scattering measurements at similar ionic strengths [Kay and Bailey, 1960], reflecting the filament-forming tendency at low salt concentrations. In contrast to the result at physiological salt, where essentially all TM was recovered as tetramers (Figs. 3A and 3B) sedimentation at the low ionic strength resulted in detectable amounts of TM at the positions corresponding to dimers and monomers of TM (Fig. 3C). This indicates that the complex isolated by gel-filtration at low ionic strength is less stable. Similar to the result obtained under physiological salt conditions TM could not be detected in fractions

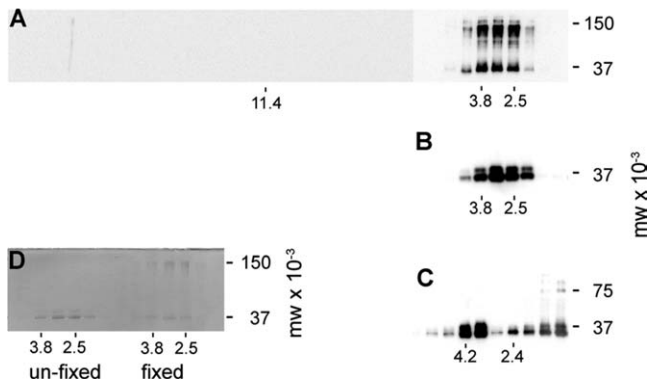


**Fig. 3. Sucrose gradient sedimentation of muscle TM at physiological and low salt conditions; effect of formaldehyde fixation. A and B**: Aliquots of TM from the peak fraction in Fig.2A, were incubated for 15 min at room temperature with formaldehyde (A; final conc. 2%) or with running buffer only (B), prior to sedimentation in sucrose gradients (5–20% in 10 mM $KPO_4$, 150 mM KCl; 1 mM DTT). **C**: non-fixed TM from the peak fraction in Fig.2B analysed after sucrose gradient sedimentation in low salt (10 mM $KPO_4$ pH 7.4, 1 mM DTT) as in B. Fractions were collected, precipitated and analyzed by Western Blot, using antibody Tm 311. Numbers below each panel refer to S-values where 11.4 denotes the catalase position. Panel A, shows the complete sedimentation profile, while B and C are cut and show TM containing fractions only. **D**: SDS-PAGE analysis (10% acrylamide) of fractions 27–33 (A and B) without prior precipitation; the gel was stained with Coomassie Brilliant Blue.

**Table II. Molecular Weight of Tropomyosin Assemblies**

| Protein | KCl (mM)[a] | I (M) | $R_s$ (nm) | S-value | MW | Gene | Variable exons [26] |
|---|---|---|---|---|---|---|---|
| Sk TM | 0 | 0.06 | 9.2 | 4.2 | 160,000 | α/β | 1A/2B/6B/9A |
| Sk TM | 150 | 0.21 | 8.2 | 3.8 | 130,000 | | |
| Sk $TM_{fix}$ | 150 | 0.21 | 8.2 | 3.8 | 130,000 | | |
| TM 1 | 80 | 0.14 | 8.3 | 3.6 | 126,000 | β | 1A/2B/6A/9D |
| TM $1_{fix}$ | 80 | 0.14 | 8.3 | 3.5 | 122,000 | | |
| TM $1_{cell\ extract}$ | 150 | 0.21 | 8.4 | 3.8[b] | 134,000 | | |
| TM $3_{cell\ extract}$ | 150 | 0.21 | 8.4 | 3.8[b] | 134 000 | α | 1A/2B/6B/9D |
| TM $4_{cell\ extract}$ | 150 | 0.21 | 7.7 | 3.8[b] | 123,000 | δ | 1A/6B/9D |
| TM 5 | 150 | 0.21 | 7.7 | 3.2 | 104,000 | γ | 1B/6A/9D |
| TM 1[c] | 150 | 0.21 | 8.3 | 3.6 | 126,000 | β | 1A/2B/6A/9D |

[a]Added to 10 mM $KPO_4$ pH 7.4, 1 mM DTT.
[b]80 mM KCl.
[c]Data not shown.

corresponding to higher S-values (data not shown). Attempts to determine the mw of TM at the highest ionic strength failed, as the high concentration of salt resulted in distorted sucrose gradients.

The initial characterization of TM assemblies from cell extracts was performed in 10 mM $KPO_4$ pH 7.6 and 80 mM KCl [Grenklo et al., 2008], and under these ionic conditions there is a close resemblance in the elution profile of skeletal muscle TM and non-muscle TM 1 expressed in *E. coli* (Figs. 4A and 4B). Sedimentation of TM 1 through a sucrose gradient in 10 mM $KPO_4$ pH 7.6 and 80 mM KCl resulted in the S-value 3.6 (Fig. 4D), and hence a mw range of 126,000 which corresponds to a tetramer. Fixation of TM 1 with formaldehyde prior to sedimentation resulted in a similar profile, and SDS-PAGE followed by Western Blot analysis showed significant amounts of fixed TM at a position of 125,000 (Fig. 4E). The appearance of material at approximately 90,000 is interpreted as a result of sample preparation (see above). Tropomyosin appearing at 37,000, i.e. the position for monomers, either represents TM that

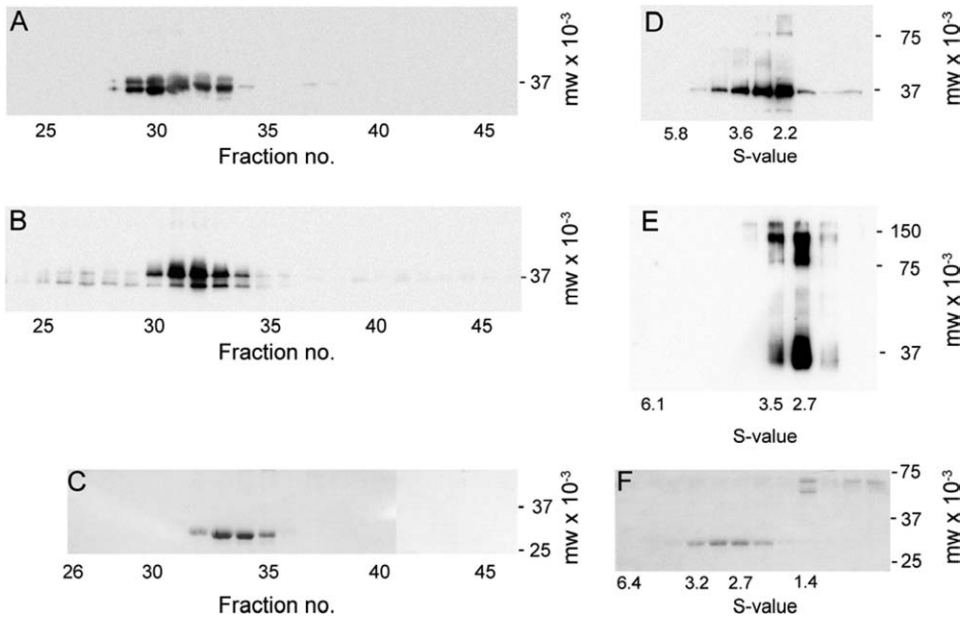


**Fig. 4. The distribution of sk-TM, TM 1 and TM 5 after gel-filtration, and of fixed and non-fixed TM 1 and non-fixed TM 5 after sucrose gradient sedimentation.** Skeletal muscle TM (**A**), TM 1 (**B**) and TM 5 (**C**) were subjected to gel filtration on Superose 6 in 10 mM $KPO_4$ pH 7.6, 80 mM KCl, 1 mM DTT (A, B), and in 10 mM $KPO_4$ pH 7.6, 150 mM KCl, 1 mM DTT (C). Fractions were analysed by SDS-PAGE followed by Western Blot using Tm311 (A, B) or by Coomassie Brilliant Blue staining (C). Panels **D–F** show the profiles, with S-values, of TM 1, non-fixed (D) and formaldehyde-fixed (E) after sucrose gradient sedimentation in 10 mM $KPO_4$ pH 7.6, 80 mM KCl, 1 mM DTT, and of TM 5 (F) after sucrose gradient sedimentation in 10 mM $KPO_4$ pH 7.6, 150 mM KCl, 1 mM DTT. The analysis was made by Western Blot using Tm311 (D, E) and by Coomassie Brilliant Blue staining (F).

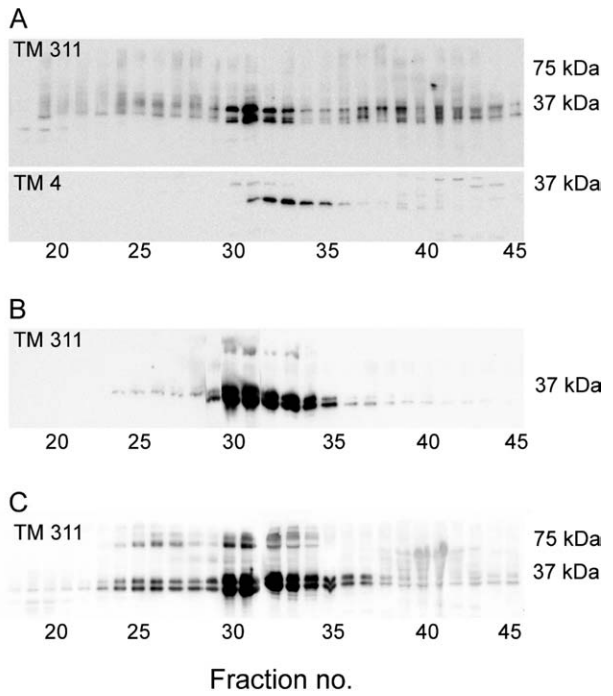


**Fig. 5. Skeletal muscle TM elutes from Superose 6 at a position, which is similar to that of non-muscle HMW TM-isoforms and is unaffected by the presence of the soluble fraction from an extract of MTLn 3 cells. A**: The distribution of HMW and LMW TM-isoforms (TM 311 and TM 4, respectively) in a cytosolic extract as shown by SDS-PAGE and Western Blot. **B**: The elution of skTM in the presence of lysis buffer as seen by SDS-PAGE and Western Blot, and **C**: the result after adding skTM to the cytosolic extract prior to chromatography. Chromatography was performed in 10 mM $KPO_4$ pH 7.4, 150 mM KCl and 1 mM DTT, and the fraction volume was 0.4 ml.

has dissociated from the fixed complex during sample preparation, or TM which was not fixed but yet distributed as tetramers during the sedimentation. A similar analysis, using 10 mM $KPO_4$ pH 7.6 and 150 mM KCl, was performed with TM 5 expressed in *E. coli*. The $R_s$ for this short TM-isoform was determined to 7.7 nm (Fig. 4C) and the S-value to 3.2 (Fig. 4F) leading to the calculated molecular weight of 104,000 i.e. close to the weight of a tetramer (112,000).

The molecular weight of TM multimers isolated from cytosolic extracts was previously estimated to 170,000–250,000 dependent on isoform type [Grenklo et al., 2008]. To address the question whether TM in cell extracts appears in larger entities than purified TM, the distribution of TM in the cytosolic fraction of cell extracts (Fig. 5A) was directly compared with muscle TM using gel chromatography, in the presence of 150 mM KCl. The distribution of the cytosolic HMW TM isoforms is shown in (Fig. 5A, upper frame; TM311); the major amounts of the protein appeared in fractions 30–33 with the peak fraction (31), corresponding to the $R_s$ 8.4 nm. In congruence with its shorter length (Table II), the LMW isoform TM 4 appeared in fractions 31–36 with the peak fraction (33) corresponding to the $R_s$ 7.7 nm (Fig. 5A, lower frame; TM 4). Thus, the $R_s$ for the HMW isoforms was similar to that obtained for muscle TM which was determined to 8.2 nm, see above. The difference in $R_s$ (8.4 vs. 8.2 nm; Table I) for the HMW isoforms compared to muscle TM was likely caused by an interaction between TM and a component of the Triton-X 100 containing lysis buffer, as pre-incubation of muscle TM with lysis buffer changed the $R_s$ to 8.4 nm (Fig. 5B).

The possibility of factor(s) present in the cytosol which could affect TM assembly was addressed by incubation of muscle TM with a cytosol extract prior to chromatography. The resulting distribution of the HMW TM isoforms is shown in (Fig. 5C), and it is concluded from the comparison of elution profiles (Figs. 5A–5C), that muscle TM was not affected by cytosolic components. The close resemblance of the elution profiles from purified TM, and HMW TM isoforms in cytosols is in line with the contention that the extracted TM multimers are essentially devoid of other components [Grenklo et al., 2008]. Still, the presence of TM in fractions 24–29 (Fig. 5C), indicate that larger organisations are also formed.

To determine the molecular weight of TM in the soluble fraction of cell extracts, the cytosol from MTLn 3 cells was subjected to sedimentation in sucrose gradients. A representative sedimentation profile (n = 3) is shown in Figure 6. The S-value obtained for TM 1, 3, and 4 was 3.8 (Figs. 6B and 6C) leading to the molecular weight 134,000 for the long isoforms, and to 123,000 for TM 4 (Table II). It is concluded from these data that the major amounts of soluble TM in cell extract is organised as tetramers. A tendency of TM 4 to distribute into fractions flanking the major portion of the protein in the sedimentation profile (Fig. 6B) might reflect interactions with components in the cell extract.

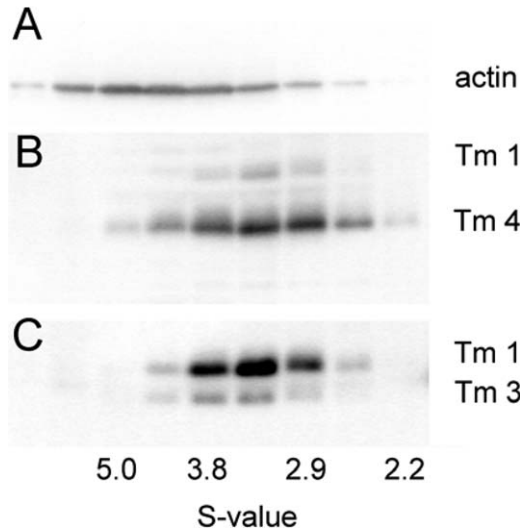


**Fig. 6. The distribution of TM and actin after sucrose gradient sedimentation of MTLn 3 cell extracts.** The soluble fraction of MTLn3 cells was subjected to sucrose gradient sedimentation in 10 mM $KPO_4$ pH 7.6, 80 mM KCl, 1 mM DTT. Fractions were analysed by SDS-PAGE followed by Western Blot. **A**: Distribution of actin using a pan-actin antibody, **B**: distribution of TM 4 and TM 1 using polyclonal TM 4 antibody (cross-reacts with TM 1), **C**: distribution of TM 1 and TM 3, using the Tm 311 antibody.

However, the influence of actin on the sedimentation profile of TM is unlikely since despite a partial overlap, the two proteins did not co-distribute (Fig. 6A).

## Discussion

This study was undertaken to determine the size of the recently discovered isoform-specific TM multimers, which appear in the soluble fraction of the cytoplasm [Grenklo et al., 2008] and implicated in the regulation of actin filament assembly. It is shown here, that skeletal muscle TM under physiological salt conditions appears as assemblies with the mw 130,000, which corresponds to a dimer of the TM-dimer usually recognized as functional TM. Hence it is concluded that native TM is a tetramer. The high degree of homogeneity of TM isolated at physiological salt concentrations (I = 0.2 M) indicated by the narrow and symmetrical shape of the corresponding peak in the chromatogram implicates that the two dimers are assembled in a precise and unique way. In contrast, at sub-physiological salt the TM organisation was characterized by increased Stokes radii, and broader peaks with shoulders were observed, implicating heterogeneities in the TM assemblies. In accordance with Kay and Bailey [1960] who determined the mw of TM at different ionic strengths, it is assumed that the assemblies obtained at the lowest ionic strengths (I = 0.03 M and 0.06 M) are formed by different numbers of TM molecules. Examination of the detailed appearance of the elution profiles reveals that the shoulder seen after chromatography in 5 mM phosphate buffer (I = 0.03 M) coincides with the peak seen with 10 mM phosphate buffer (I = 0.06 M), suggesting a mixture of assemblies in 5 mM phosphate and that one of these becomes a prominent assembly variant in 10 mM phosphate. The mw of the major fraction of TM assemblies obtained with 10 mM phosphate buffer was 160,000 as determined after sucrose gradient centrifugation, and therefore the gradual decrease in $R_s$ seen with increased concentrations of KCl in 10 mM phosphate buffer likely reflects differences in packing rather than in number of molecules. While the two TM-polypeptides forming dimers are associated in register [Lehrer, 1975; Stewart, 1975], it is unclear how the dimers in turn form tetramers. Cryo-electron microscopy and x-ray diffraction of TM in so called Bailey crystals show a mesh of filaments crossing each other, where each arm contains two TM dimers aligned with blunt ends [Phillips et al., 1986; Cabral-Lilly et al., 1991]. On the other hand studies of crystals obtained under different conditions demonstrate a packing of the TM-dimers in a staggered, anti-parallel way with approximately 50% overlap [Whitby and Phillips, 2000]. This suggests a complex dependence of TM organization on the assembly conditions.

The conclusion here that native TM is a tetramer is supported by results obtained by different methods during the early biochemical and biophysical characterization of TM [Tsao et al., 1951; Kay and Bailey, 1960; Woods, 1967]. Tsao et al. [1951] showed that the mw is 135,000 at I = 0.1 M; 110,000 at I = 0.2 M, and 64,500 at I = 1.1 M, and that the large assemblies obtained at I = 0.1 M disintegrated to half the size (mw 52,000–61,000) by addition of urea or at extreme pH; Woods [1967] observed a variability in TM-assembly and concluded that "TM is heterogeneous in aqueous buffers at neutral pH and at all salt concentrations, and consists of an associating system which at low concentrations dissociates to a molecular weight of approximately 68,000"; and Coté et al. [1978] reported a mw of 140,000–160,000 for skeletal α-TM at I = 0.1 M. Finally, in a study similar to ours, the mw of TM isolated from REF cells in the presence of 0.6 M NaCl was determined to 105,000 and 87,000 for the HMW and LMW isoforms, respectively [Matsumura and Yamashiro-Matsumura, 1985].

These early efforts, aimed to determine the minimal assembly form of TM, lead to identification of the coiled-coil structure of the dimer and its head-to tail assembly along actin filaments [Caspar et al., 1969; Greenfield et al., 2006], while the observation of the larger TM assemblies was apparently not recognized during studies that followed possibly due to the strong focus on understanding the role of TM in muscle cells. Later studies on tropomyosin dimerization showed that the alternatively spliced exons contain the information that determine formation of homo- or heterodimers [Gimona et al., 1995]. In view of recent studies of TM organization, distribution and isoform-dependent functional specializations in non-muscle cells, the existence of alternative TM assembly forms must be taken into consideration for understanding actin control and dynamics during non-muscle cell motility [Bryce et al., 2003; Creed et al., 2008; Gunning et al., 2008; Bugyi et al., 2009]. The isoform specific "dots" of TM observed in lamellipodia might consist of tetramers, but could also be larger entities assembled by factor(s) notwithstanding the Triton X-100 extraction. The time-dependent and isoform-specific changes in the soluble TM pools concomitant to stimulation of cells [Grenklo et al., 2008], suggest that tetramers are released upon cell activation and contribute to the regulation of the rapid and polymerization-driven advancement of the lamellipodia, similar to the situation in fission yeast where TM is implicated in formin driven actin polymerization [Skau et al., 2009]. At present it is unclear how the tetramers function in this context; as shown here this assembly form represents an actin independent organization of the protein. This study includes TM encoded by four different genes and forming homodimers and heterodimers, as well as TM in cell extracts, and therefore strongly implicates the tetramer as a general assembly form of the protein.

### Acknowledgments

We gratefully acknowledge Rolf Eriksson and Arne Holmgren, MBB, KI, for expert assistance and support with sucrose gradients, and Ingemar Ernberg, MTC, KI, for generously sharing space and mind with us in his laboratory. This work was made possible through generous grants to UL from Nancy Lurie Marks Family Foundation, The Swedish Cancer Society and from the Swedish Research Council.

## References


Bach CT, Creed S, Zhong J, Mahmassani M, Schevzov G, Stehn J, Cowell LN, Naumanen P, Lappalainen P, Gunning PW, O'Neill GM. 2009. Tropomyosin isoform expression regulates the transition of adhesions to determine cell speed and direction. Mol Cell Biol 29 (6): 1506–1514.

Bailey K. 1948. Tropomyosin: a new asymmetric protein component of the muscle fibril. Biochem J 43 (2): 271–9.

Blikstad I, Carlsson L. 1982. On the dynamics of the microfilament system in HeLa cells. J Cell Biol 93 (1): 122–128.

Brachmann SM, Yballe CM, Innocenti M, Deane JA, Fruman DA, Thomas SM, Cantley LC. 2005. Role of phosphoinositide 3-kinase regulatory isoforms in development and actin rearrangement. Mol Cell Biol 25 (7): 2593–2606.

Bryce NS, Schevzov G, Ferguson V, Percival JM, Lin JJ, Matsumura F, Bamburg JR, Jeffrey PL, Hardeman EC, Gunning P, Weinberger RP. 2003. Specification of actin filament function and molecular composition by tropomyosin isoforms. Mol Biol Cell 14 (3): 1002–1016.

Bugyi B, Didry D, Carlier MF. 2010. How tropomyosin regulates lamellipodial actin-based motility: a combined biochemical and reconstituted motility approach. Embo J 29: 14–26.

Cabral-Lilly D, Phillips GN Jr, Sosinsky GE, Melanson L, Chacko S, Cohen C. 1991. Structural studies of tropomyosin by cryoelectron microscopy and x-ray diffraction. Biophys J 59 (4): 805–814.

Carlier MF, Pantaloni D. 2007. Control of actin assembly dynamics in cell motility. J Biol Chem 282 (32): 23005–23009.

Caspar DL, Cohen C, Longley W. 1969. Tropomyosin: crystal structure, polymorphism and molecular interactions. J Mol Biol 41 (1): 87–107.

Chiarugi P, Fiaschi T. 2007. Redox signalling in anchorage-dependent cell growth. Cell Signal 19 (4): 672–682.

Chinkers M, McKanna JA, Cohen S. 1979. Rapid induction of morphological changes in human carcinoma cells A-431 by epidermal growth factors. J Cell Biol 83 (1): 260–265.

Cote G, Lewis WG, Smillie LB. 1978. Non-polymerizability of platelet tropomyosin and its NH2- and COOH-terminal sequences. FEBS Lett 91 (2): 237–241.

Creed SJ, Bryce N, Naumanen P, Weinberger R, Lappalainen P, Stehn J, Gunning P. 2008. Tropomyosin isoforms define distinct microfilament populations with different drug susceptibility. Eur J Cell Biol 87 (8–9): 709–720.

Dalle-Donne I, Giustarini D, Rossi R, Colombo R, Milzani A. 2003. Reversible S-glutathionylation of Cys 374 regulates actin filament formation by inducing structural changes in the actin molecule. Free Radic Biol Med 34 (1): 23–32.

Evangelista M, Pruyne D, Amberg DC, Boone C, Bretscher A. 2002. Formins direct Arp2/3-independent actin filament assembly to polarize cell growth in yeast. Nat Cell Biol 4 (3): 260–269.

Fratelli M, Demol H, Puype M, Casagrande S, Eberini I, Salmona M, Bonetto V, Mengozzi M, Duffieux F, Miclet E, Bachi A, Vandekerckhove J, Gianazza E, Ghezzi P. 2002. Identification by redox proteomics of glutathionylated proteins in oxidatively stressed human T lymphocytes. Proc Natl Acad Sci USA 99 (6): 3505–3510.

Gimona M, Watakabe A, Helfman DM. 1995. Specificity of dimer formation in tropomyosins: influence of alternatively spliced exons on homodimer and heterodimer assembly. Proc Natl Acad Sci USA 92 (21): 9776–9780.

Goley ED, Welch MD. 2006. The ARP2/3 complex: an actin nucleator comes of age. Nat Rev Mol Cell Biol 7 (10): 713–726.

Greenfield NJ, Huang YJ, Swapna GV, Bhattacharya A, Rapp B, Singh A, Montelione GT, Hitchcock-DeGregori SE. 2006. Solution NMR structure of the junction between tropomyosin molecules: implications for actin binding and regulation. J Mol Biol 364 (1): 80–96.

Grenklo S, Hillberg L, Zhao Rathje LS, Pinaev G, Schutt CE, Lindberg U. 2008. Tropomyosin assembly intermediates in the control of microfilament system turnover. Eur J Cell Biol 87 (11): 905–920.

Gunning PW, Schevzov G, Kee AJ, Hardeman EC. 2005. Tropomyosin isoforms: divining rods for actin cytoskeleton function. Trends Cell Biol 15 (6): 333–341.

Gunning P, O'Neill G, Hardeman E. 2008. Tropomyosin-based regulation of the actin cytoskeleton in time and space. Physiol Rev 88 (1): 1–35.

Hall A. 2005. Rho GTPases and the control of cell behaviour. Biochem Soc Trans 33 (Pt 5): 891–895.

Hillberg L, Zhao Rathje LS, Nyåkern-Meazza M, Helfand B, Goldman RD, Schutt CE, Lindberg U. 2006. Tropomyosins are present in lamellipodia of motile cells. Eur J Cell Biol 85 (5): 399–409.

Ishikawa R, Yamashiro S, Matsumura F. 1989. Annealing of gelsolin-severed actin fragments by tropomyosin in the presence of Ca2+. Potentiation of the annealing process by caldesmon. J Biol Chem 264 (28): 16764–16770.

Kay CM, Bailey K. 1960. Light scattering in solutions of native and guanidinated rabbit tropomyosin. Biochim Biophys Acta 40: 149–156.

Laemmli UK. 1970. Cleavage of structural proteins during the assembly of the head of bacteriophage T4. Nature 227 (5259): 680–685.

Lai FP, Szczodrak M, Block J, Faix J, Breitsprecher D, Mannherz HG, Stradal TE, Dunn GA, Small JV, Rottner K. 2008. Arp2/3 complex interactions and actin network turnover in lamellipodia. Embo J 27 (7): 982–992.

Lassing I, Lindberg U. 1988. Evidence that the phosphatidylinositol cycle is linked to cell motility. Exp Cell Res 174 (1): 1–15.

Lassing I, Schmitzberger F, Björnstedt M, Holmgren A, Nordlund P, Schutt CE, Lindberg U. 2007. Molecular and structural basis for redox regulation of beta-actin. J Mol Biol 370 (2): 331–348.

Le Clainche C, Carlier MF. 2008. Regulation of actin assembly associated with protrusion and adhesion in cell migration. Physiol Rev 88 (2): 489–513.

Lehrer SS. 1975. Intramolecular crosslinking of tropomyosin via disulfide bond formation: evidence for chain register. Proc Natl Acad Sci USA 72 (9): 3377–3381.

Lindberg U, Schutt CE, Goldman RD, Nyåkern-Meazza M, Hillberg L, Rathje LS, Grenklo S. 2008. Tropomyosins regulate the impact of actin binding proteins on actin filaments. Adv Exp Med Biol 644: 223–231.

Martin RG, Ames BN. 1961. A method for determining the sedimentation behavior of enzymes: application to protein mixtures. J Biol Chem 236: 1372–1379.

Matsumura F, Yamashiro-Matsumura S. 1985. Purification and characterization of multiple isoforms of tropomyosin from rat cultured cells. J Biol Chem 260 (25): 13851–13859.

Mejillano MR, Kojima S, Applewhite DA, Gertler FB, Svitkina TM, Borisy GG. 2004. Lamellipodial versus filopodial mode of the actin nanomachinery: pivotal role of the filament barbed end. Cell 118 (3): 363–373.

Mellstroom K, Höglund AS, Nistér M, Heldin CH, Westermark B, Lindberg U. 1983. The effect of platelet-derived growth factor on morphology and motility of human glial cells. J Muscle Res Cell Motil 4 (5): 589–609.

Moldovan L, Mythreye K, Goldschmidt-Clermont PJ, Satterwhite LL. 2006. Reactive oxygen species in vascular endothelial cell motility. Roles of NAD(P)H oxidase and Rac1. Cardiovasc Res 71 (2): 236–246.

Nyakern-Meazza M, Narayan K, Schutt CE, Lindberg U. 2002. Tropomyosin and gelsolin cooperate in controlling the microfilament system. J Biol Chem 277 (32): 28774–28779.

Ono S, Ono K. 2002. Tropomyosin inhibits ADF/cofilin-dependent actin filament dynamics. J Cell Biol 156 (6): 1065–1076.

Phillips GN Jr, Fillers JP, Cohen C. 1986. Tropomyosin crystal structure and muscle regulation. J Mol Biol 192 (1): 111–131.

Renault L, Bugyi B, Carlier MF. 2008. Spire and Cordon-bleu: multifunctional regulators of actin dynamics. Trends Cell Biol 18 (10): 494–504.

Siegel LM, Monty KJ. 1966. Determination of molecular weights and frictional ratios of proteins in impure systems by use of gel filtration and density gradient centrifugation. Application to crude preparations of sulfite and hydroxylamine reductases. Biochim Biophys Acta 112 (2): 346–362.

Silacci P, Mazzolai L, Gauci C, Stergiopulos N, Yin HL, Hayoz D. 2004. Gelsolin superfamily proteins: key regulators of cellular functions. Cell Mol Life Sci 61 (19–20): 2614–2623.

Skau CT, Neidt EM, Kovar DR. 2009. Role of tropomyosin in formin-mediated contractile ring assembly in fission yeast. Mol Biol Cell 20 (8): 2160–2173.

Smillie LB. 1982. Preparation and identification of alpha- and beta-tropomyosins. Methods Enzymol 85 (Pt B): 234–241.

Stewart M. 1975. Tropomyosin: evidence for no stagger between chains. FEBS Lett 53 (1): 5–7.

Sundaresan M, Yu ZX, Ferrans VJ, Irani K, Finkel T. 1995. Requirement for generation of $H_2O_2$ for platelet-derived growth factor signal transduction. Science 270 (5234): 296–299.

Takenawa T, Suetsugu S. 2007. The WASP-WAVE protein network: connecting the membrane to the cytoskeleton. Nat Rev Mol Cell Biol 8 (1): 37–48.

Tsao TC, Bailey K, Adair GS. 1951. The size, shape and aggregation of tropomyosin particles. Biochem J 49 (1): 27–36.

Wang YL. 1985. Exchange of actin subunits at the leading edge of living fibroblasts: possible role of treadmilling. J Cell Biol 101 (2): 597–602.

Wawro B, Greenfield NJ, Wear MA, Cooper JA, Higgs HN, Hitchcock-DeGregori SE. 2007. Tropomyosin regulates elongation by formin at the fast-growing end of the actin filament. Biochemistry 46 (27): 8146–8155.

Whitby FG, Phillips GN Jr. 2000. Crystal structure of tropomyosin at 7 Angstroms resolution. Proteins 38 (1): 49–59.

Woods EF. 1967. Molecular weight and subunit structure of tropomyosin B. J Biol Chem 242 (12): 2859–2871.